PERGAMON

International Journal of Impact Engineering 26 (2001) 289–298

INTERNATIONAL JOURNAL OF IMPACT ENGINEERING

www.elsevier.com/locate/ijimpeng

AN EXTENSION OF THE UMIN MODEL FOR CUTOFF OF HIGH PRECISION JETS

STEVEN L. HANCOCK

Consultant, Primex Technologies, P.O. Box 2055, San Leandro, CA 94577

Abstract— The mechanical processes leading to the cutoff of penetration of a shaped charge jet are still poorly understood. Eventually, high resolution 3D computer simulations may help resolve the mechanisms involved, but currently empirical models are required for practical work. The present work is concerned specifically with modeling the cutoff of high precision jets in metal targets. Motivated by a lack of success with existing jet penetration models when applied at very low drift velocities, the present work investigates a new approach. A new drift velocity term is added to one of the oldest and simplest models, the UMIN model. The new model is illustrated by applying it to the BRL 3.3 inch standard test charge, and the results are encouraging.

Keywords: breakup, cutoff, drift, jet, penetration, shaped charge, standoff, CALE, UMIN

NOTATION

b	drift coefficient for extended model	c_b	breakup parameter, τ_b/τ_b
g	gap between particles	L	particle length
M	cumulative mass	P	penetration
$r_b(v)$	jet radius at breakup	S	standoff distance to target
t	time	$t_b(v)$	breakup time
$t_{vo}(v)$	t of local virtual origin	U	average penetration rate
U_0	rate coefficient for extended model	U_{min}	penetration rate at cutoff
v	jet velocity	v_c	jet cutoff velocity
v_d	radial drift velocity	z	axial distance from device
$z_{vo}(v)$	z of local virtual origin	γ	$(\rho_t/\rho_j)^{1/2}$
δ_r	radial drift distance	ρ_j	jet density
ρ_t	target density	$\tau_b(v)$	local breakup time duration

INTRODUCTION

When a shaped charge device is fired at a stack of steel target blocks, the velocity of the last particle to contribute to increasing the hole depth is called the "cutoff velocity". Although the cutoff velocity varies somewhat from shot to shot, the variations can be surprisingly small for high precision jets, with penetrations often repeatable to within a couple of jet particle lengths. The jet cutoff process is still very poorly understood, although it is generally thought to be triggered by lateral interactions of jet particles with the target material. When the cutoff velocity for a given device is tabulated as a function of the standoff distance to the target, it is found to increase

0734-743X/01/$ - see front matter
PII: S0734-743X(01)00095-1

Table 1. Cutoff velocity for best shots of the 3.3 inch BRL precision standard charge [1].

Standoff, CD's	2	5	8	12	15	20	25
v_c km/s	3.04	3.61	4.01	4.31	4.77	5.69	6.55

monotonically. An example of such a table is displayed in Table 1. In this table, standoff distance is normalized to the charge diameter (CD). This data will be discussed later in this paper. At a sufficiently great distance, the cutoff velocity approaches the velocity of the jet tip, and penetration falls to a very low level. (Penetration does not fall to zero, because individual particles will still cause surface cratering, but jet particles below the cutoff velocity seem unable to act in concert to deepen a single hole). To someone unfamiliar with the jet cutoff effect, it can be quite surprising to see a radiograph of an apparently straight jet of particles which are almost completely ineffective against steel below a velocity of, say, 6 km/s, if the steel is beyond a certain standoff distance.

One way to measure cutoff velocity is with timing screens placed between target blocks (e.g. Held, [2]). For precision charges, cutoff velocities obtained in this manner are normally in good agreement with estimates based upon applying hydrodynamic penetration assumptions to the jet from the tip down to the cutoff particle (e..g. Held, [3]). (The term "precision" will be used here to indicate jets which, through material selection, precision machining, and assembly techniques, have consistently low drift velocities, say below about 10 m/s.) This implies that the penetration process is efficient down to cutoff, and then terminates rather abruptly.

Cutoff seems to be an inherently three-dimensional effect, and eventually high resolution 3D calculations should be able to clarify the mechanisms involved, but for now simplified penetration models are required. A variety of simplified jet penetration models have been proposed; for a review, see Walters and Zukas, [4]. Most models assume that the jet consumption obeys a hydrodynamic penetration rule, but they vary widely in the treatment of the termination of penetration. The models may be broadly categorized as either empirical or geometrical. An example of an empirical model is the UMIN cutoff model of DiPersio, Simon, and Merindino (DSM) [1]. Examples of geometrical models can be found in [5]-[8]. The geometrical models generally assume that particles have some statistical distribution of drift velocities, and in some cases rotation rates, and that a particle is unable to reach the bottom of the hole when it contacts the sidewall.

It is almost always possible to find a set of drift velocities which allow a drift-based model to match any particular set of data, but it is very difficult to demonstrate the validity of such a model. This is because drift velocities are different in each shot, so it would be necessary to make simultaneous drift and cutoff velocity measurements for a single shot. This is a very difficult task, because accurate drift measurements normally require a long free flight of the jet, particularly for high precision jets.

The present paper explores a new simple empirical cutoff model. It was developed in an attempt to overcome some difficulties encountered with a geometric model at low drift velocities. The problem, which may be common to other geometrical models, is related to the fact that a geometric model, when tested with zero drift, will typically predict "ideal" penetration, which is a theoretical limiting penetration generally far above actual measurements, particularly at long standoff distances. The explanation normally given for the discrepancy is that real jets always have asymmetries and drift which prevent ideal penetration from being reached. Nevertheless, if ideal penetration is the limiting state for a geometrical model, then it will converge to this state as the drift velocity is decreased. The problem which was encountered was that the rate of convergence to ideal penetration seemed to be much too great, resulting in excessive penetration estimates for low drift jets. This is difficult to prove, because of the lack of simultaneous penetration and drift data, but the problem was significant enough to warrant examining an alternative approach.

One possible source of error in some geometrical models has to do with the cylindrical cavity expansion model commonly used to model hole growth. This probably gives a reasonable de-

scription of hole growth during the continuous mode of penetration, but cutoff of precision jets nearly always occurs in the particulated mode, which produces very different hole characteristics, a fact well known to experimentalists (e.g. Held, [9]). In continuous penetration, the cavity wall is relatively smooth, whereas in particulated penetration, the penetration progresses with a series of "bubbles" in the target, each being caused by a single particle. These bubbles may be difficult to discern in tests of jets with high drift velocities, having been eroded away, but the hallmark of a low drift shot is a long chain of these bubbles. These bubbles are connected by constrictions which are much narrower than the average hole diameter. Particles traveling down the hole will strike these constrictions first, rather than the main cavity wall, and yet they are not typically included in a geometric model.

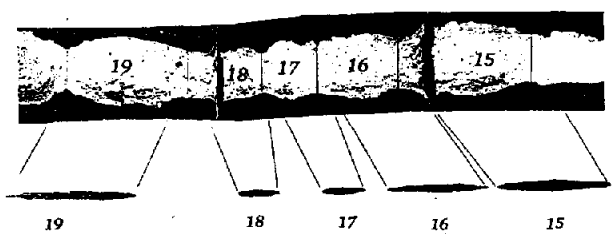

Fig. 1. Bubbles formed in an RHA steel target. The direction of jet travel is from left to right; the direction of target penetration is from right to left. The jet particles are molybdenum traveling at about 9 km/s. The breaks in bubbles 15 and 18 are due to target block interfaces.

Figure 1 shows a sequence of jet particles and the bubbles they produced. This data is from a test by Boeka [10] in which a jet was captured on film before penetrating a target, and the individual jet particles were matched up with the bubbles that they created in the target. Hydrocode calculations were made of this penetration event and gave good agreement on the lengths and maximum diameters of the bubbles. They also showed that the openings between the bubbles are even smaller than in the sectioned target blocks, probably because the initial fine features of target blocks are later eroded away by jet material, perhaps as part of the cutoff process.

A MODIFICATION OF THE UMIN MODEL TO INCLUDE RADIAL DRIFT

To avoid the difficulties and uncertainties of detailed geometric modeling, an abstract approach will be taken here. It will be assumed that the cutoff effect is due to an obscure but essentially repeatable process. It should then be possible to develop a "black box" function which describes its overall effect as a function of the key parameters. As a starting point, consider the idealized situation of quasi-steady state penetration by a train of identical particles of some arbitrary shape, each having a velocity v, length L, radius r_b, separation gap g, and a small radial drift distance δ_r. The direction of this drift, in the plane perpendicular to the direction of flight, will be assumed to be essentially random. The penetration is assumed to be deep enough that there are no entrance effects. It is hypothesized that under these circumstances there is a well-defined cutoff velocity v_c such that penetration proceeds in a stable manner if $v > v_c$ and becomes unstable and is interrupted otherwise. If this is true, then there should be some function such that

$$f(v_c, L, g, r_b, \delta_r, \text{particle shape, material properties}) = 0. \tag{1}$$

While such a function might be very complicated, it should be possible to develop a useful approximation to it.

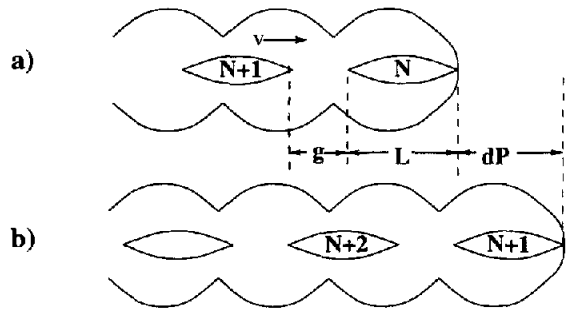

Fig. 2. Illustration of particle impact for computing average penetration rate.

For reasons which will become clear, the minimum penetration rate (UMIN) model (DSM, [1]) makes a practical starting point for developing this function. This model postulates that cutoff occurs when the average penetration rate falls below a constant, U_{min}, whose value has been shown to correlate well with target strength. In particulated penetration, the UMIN model can be shown to have the form $f(v_c, g/L, \text{material properties}) = 0$. In other words, it includes the effects of inter-particle gaps but not of radial drift.

To show this, we need to express the average penetration rate in terms of the inter-particle gap. Consider the train of identical particles shown in figure 2, in which particle n is starting to penetrate in (a) and particle $n+1$ is starting to penetrate in (b). The time interval between the two figures is $\Delta t = (g + L + \Delta P)/v$, and the hole bottom has advanced by a distance of ΔP, so the average penetration rate U can be written

$$U = \Delta P/\Delta t = \frac{v}{1 + \gamma(1 + g/L)}, \tag{2}$$

where $\gamma = L/\Delta P$, and equals $(\rho_t/\rho_j)^{1/2}$ if hydrodynamic penetration is assumed. When g/L is zero, U equals the continuous hydrodynamic penetration rate, and as g/L increases, U decreases. During penetration by a stretching jet, the value of g/L of the particle currently forming the hole bottom increases, and the value of v decreases, so that eventually the value of U falls below the critical constant, which implies cutoff according to the UMIN model. To show the model in the form of Eqn. 1, we can equate this expression to the constant U_{min} and set $v = v_c$, giving

$$f(v_c, g/L, \gamma, U_{min}) = \frac{v_c}{1 + \gamma(1 + g/L)} - U_{min} = 0. \tag{3}$$

In a sense, the UMIN model is the extreme opposite of a geometric penetration model, because the UMIN model relies completely on the term g/L to reduce penetration with distance, whereas a geometric cutoff model relies almost completely on drift, δ_r, to reduce penetration with distance. In reality, both terms are probably important. The importance of lateral drift is well known; the gap is also important because the formation of constrictions between bubbles in the target depends upon it, and in addition, the greater the gap, the more likely it is that target ejecta can interfere with particle flight.

What makes the UMIN model a good starting point for an empirical low-drift model is that it defines an experimental first approximation to the functional behavior of cutoff at low drift velocities. This is because the DSM authors collected data from repeated penetration tests and fit only the highest penetration results with the model. With enough precision shots, this procedure should converge to an experimentally defined low-drift cutoff limit. Although they fired relatively few shots, their results at least give a hint at the limiting behavior of cutoff at very low drift. They recognized, but did not attempt to model, the fact that random drift may produce penetration

results below the prediction of the constant U_{min} condition. Later attempts were made to employ the UMIN model as a general cutoff law, rather than as a low-drift limit, sometimes with erratic results and sometimes with some success (Majerus and Scott,[14]; Shear *et al.* [15]).

The idea of the present paper is to extend U_{min} to be a function of δ_r, thereby building a drift model which has the U_{min} model as its zero-drift limit, rather than ideal penetration. To insure that the model scales properly with size, the extended model must normalize δ_r to an appropriate dimension. The choice here is to use the jet particle breakup radius, r_b, because, considering the narrow constrictions between the bubbles formed in particulated penetration, it is likely that drift distances on the order of r_b are quite significant for the cutoff process. With this assumption, the functional dependence is $U_{min} = U_{min}(\delta_r/r_b)$. With the additional assumption that a first-order Taylor series expansion can be made for small drift velocities, the model can be written

$$U_{min} = U_0\,(1 + b\delta_r/r_b) \tag{4}$$

where U_0 and b are constants. This equation extends the empirical function, Eqn. 3, to have the form $f(v_c, g/L, \delta_r/r_b, \gamma, U_0) = 0$. The model is still independent of L/r_b, particle shape, and perhaps additional relevant material properties, but it will be shown that the addition of the drift term can significantly extend the usefulness of the UMIN model.

EXTENSION TO STRETCHING JETS

The preceding discussion concerned a steady state penetration process. To apply the model to a stretching jet, it will be assumed that the jet passes through a sequence of nearly steady states to which the model can be applied.

A breakup model is required for a stretching jet. This is a separate modeling issue, but to illustrate the cutoff model, the present work assumes that the breakup time duration, $\tau_b(v)$, and breakup radius, $r_b(v)$, are proportional along the entire jet with the proportionality constant, c_b. This assumption can be written

$$\tau_b(v) = r_b(v)/c_b. \tag{5}$$

The additional assumption of incompressibility implies the following relationship, which can be used to compute $\tau_b(v)$ from the slope of the cumulative mass curve (e.g. Hancock, [12]),

$$\pi\rho_j c_b^2 \tau_b^3 = -dM/dv. \tag{6}$$

(For clarity, from this point on the functional dependence on v of local jet properties such as τ_b and r_b will be assumed but not indicated).

It is important to make a distinction between a global time scale, t, which may have an arbitrary zero reference point, and the local breakup time duration, τ_b. For a stretching jet it is always possible to determine a local virtual origin in space and time, z_{vo} and t_{vo}, and it will in general be different for each element of the jet. The assumption to be made here is that the clock for breakup starts at the local virtual origin time, so that $\tau_b = t_b - t_{vo}$.

The variation in time of the radial drift distance, δ_r, needs to be specified. A variety of assumptions can be made, but here it will be assumed that the drift occurs according to a drift velocity v_d beginning at the local virtual origin, so that

$$\delta_r = v_d(t - t_{vo}). \tag{7}$$

An expression for the penetration rate in a stretching, particulated jet can be obtained as follows. The distance between two jet elements separated by a small velocity interval Δv at time t is $\Delta z = (t - t_{v0})\Delta v$, so that at breakup, the intervening jet length will be $L = \tau_b \Delta v$. After breakup, ignoring the effects of finite particle sizes and the associated local equilibrium processes, the increase in Δz

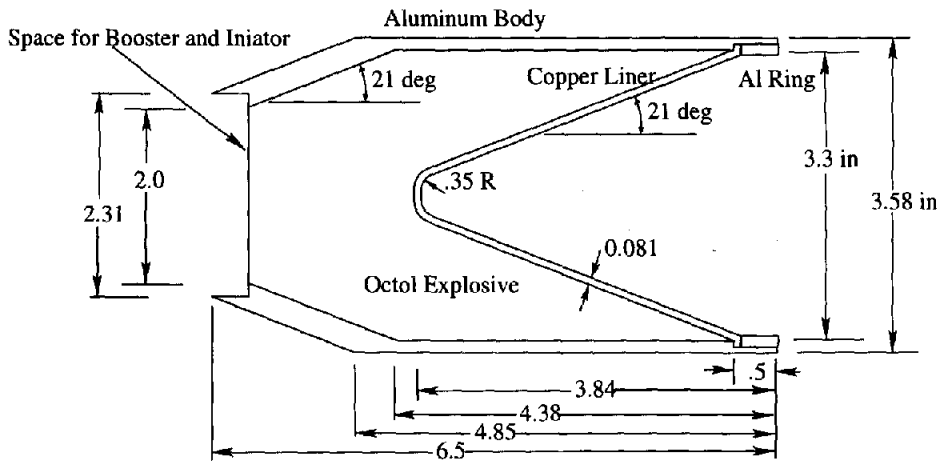

Fig. 3. The BRL 3.3 inch standard charge, from [1]. Dimensions are in inches (1 in = 25.4 mm).

Table 2. BRL 3.3 inch standard charge penetration data, from DSM, [1]. Only the best results at 15 and 20 CD's were reported.

Standoff, CD's	Penetration, inches (1 inch = 25.4 mm)	
	Precision charge	Non-precision charge
2	15.7, 16.2, 15.5, 16.0, 15.6	15.3, 12.8, 15.1, 15.0, 16.0
5	17.6, 18.8, 18.2, 18.6, 18.2	10.5, 14.8, 8.6
8	17.8, 18.4, 18.8, 17.7	8.0, 5.2, 8.6, 8.3, 8.4
12	17.0, 14.1, 14.5, 17.3	4.8, 6.4, 2.7, 7.0, 6.7
15	15.3 (best)	
20	11.3 (best)	
25	2.5, 5.0, 5.6, 6.0, 7.6	2.0, 3.3, 0.8, 1.2

will be accommodated by a gap growth of $g = (t - t_b)\Delta v$. Substituting these expressions for L and g into Eqn. 2 gives the average penetration rate after particulation as

$$U = v/[1 + \gamma(t - t_{vo})/\tau_b], \tag{8}$$

where t is the hole-bottom time of the particle with velocity v.

APPLICATION TO THE BRL 3.3 INCH STANDARD CHARGE

The UMIN model was originally developed to fit the data collected for the BRL 3.3 inch (83.82 mm) standard charge, Fig. 3, so it is appropriate to compare this extension of the model with the same data, which is shown in Table 2.

The CALE hydrocode (Tipton, [11]) was used to find the cumulative mass curve, yielding the curve shown in Figure 4. Also shown is a smooth analytical fit to the calculated mass profile. This fit was used to make the small extrapolation from the calculated tip velocity, 8.17 km/s, to the reported experimental value of 8.3 km/s. The cumulative mass profile may be described as being almost linear from the tip down to about 5.5 km/s, and then highly curved down to about 4 km/s, and then nearly linear again down to 2 km/s.

The charge has a reported breakup time of 103 μs and constant breakup radius of 1 mm. In the front, nearly linear section of the jet, a breakup time of 103 μs corresponds to a computed

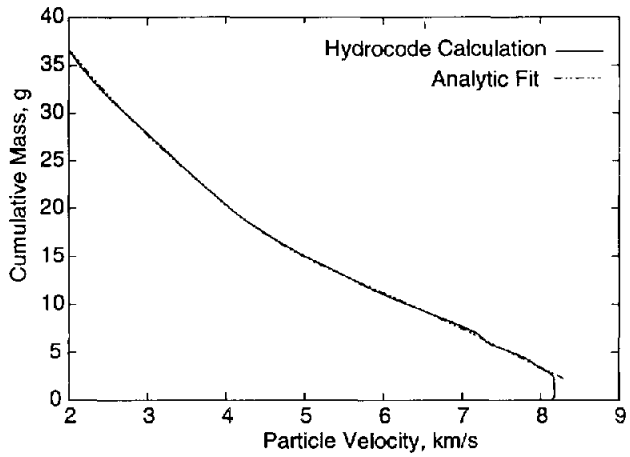

Fig. 4. Cumulative mass for the BRL 3.3 inch standard charge, and a smooth fit.

breakup radius of 1.15 mm, in fair agreement with this description. It is not possible to match both the reported breakup radius and breakup time below about 5.5 km/s, however, so a compromise is required. In the present work, the value of the breakup model parameter c_b will be taken to be the value found in the front section of the jet.

Since the drift velocities in the original tests are unknown, it isn't possible to assign accurate values to the two cutoff model parameters, U_0 and b. Nevertheless, some approximate values can be used to illustrate the use of the model. Since U_0 defines the zero-drift condition, it must be chosen such that the corresponding zero-drift penetration curve is an upper bound on all test data. The original peak penetration in the DSM data was modeled with a constant value of U_{min}=1000 m/s. Based upon the cumulative mass fit used here, the maximum possible value of U_0 is about 1100 m/s. Since it is unlikely that any of the shots actually reached zero drift, the somewhat lower value of 900 m/s will be used here, which leaves a little margin between the zero drift curve and the peak of the data. The parameter b will be taken to have the value 0.5, which is estimated to produce drift velocities with the correct order of magnitude, and will serve to illustrate the model.

Figure 5 compares the model predictions using these parameters with the test data. The penetration depths were computed assuming hydrodynamic penetration, $dP = dL/\gamma$, where dL is the length of a jet element at the time it reaches the hole bottom. The non-precision data is included in the plot along with the precision data, even though the primary aim of the model is to treat the precision data. The upper curve is the zero-drift penetration curve, and its height is controlled by the value of U_0. Also plotted are curves for several drift values. The initial rise in the curves is due to jet stretching, and the decrease with standoff distance is controlled by the increase of particle drift as well as the increase of particle gaps with distance.

It can be seen that the peak of the precision data falls largely between the 2 m/s and 4 m/s drift curves. To show the comparison in numerical form, Table 3 compares the cutoff velocities for this drift range with the cutoff data previously shown as Table 1. The agreement is fairly good, and it illustrates how cutoff velocity information can be sometimes be compressed into simpler drift velocity information with the help of this model.

A limitation on the model is that it predicts zero penetration when the predicted cutoff velocity exceeds the jet tip velocity. In reality, actual penetration will not fall to zero, because there will always be some surface penetration, which is different from the deep penetration mode treated by the model. This explains why the 25 CD non-precision data points are out of line (in terms of their lower apparent drift) with the rest of the non-precision data. A simple way to fix the model to account for this would be to place a reasonable lower bound on the model penetration predictions,

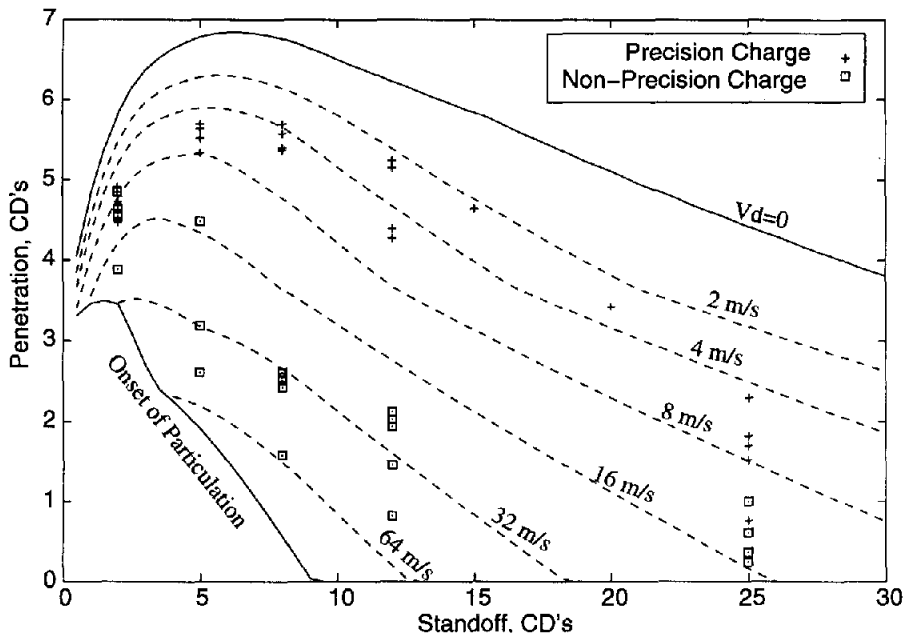

Fig. 5. Computed standoff curves for BRL 3.3 inch standard charge.

Table 3. Comparison of Cutoff Velocities, in km/s.

Standoff, CD	2	5	8	12	15	20	25
Data, peak	3.04	3.61	4.01	4.31	4.77	5.69	6.55
Model, v_d=2-4 m/s	2.75-2.90	3.35-3.59	3.76-4.04	4.25-4.75	4.71-5.21	5.39-5.89	5.88-6.41

on the order of 1 CD.

Most of the precision data lies between the 2 m/s and 8 m/s drift velocity standoff curves, whereas the non-precision data falls mainly between the 16 m/s and 64 m/s curves (with the exception noted for the non-precision 25 CD data). This suggests that the non-precision jets have drift velocities on the order of 8 times the precision jets. This is not unreasonable, based upon the published machining tolerances for these charges.

In summary, it can be seen that the model provides a simple way to correlate and interpret test data, such as the data in Table 2, even with some uncertainties in the model parameters. An effective way to use the model with test data is to determine the apparent drift velocity corresponding to the penetration of each shot. By compiling a history of such drift values, it becomes possible to predict with some confidence the range of penetration expected due to design and standoff changes.

VARIATION OF CUTOFF VELOCITY WITH DISTANCE

An interesting way to display cutoff velocity data is to follow a suggestion of Pearson [13], who showed a good correlation of cutoff data among a number of shaped charge devices by cross-plotting cutoff velocity with the flight distance of the cutoff particle, normalized to particle diameter. The present model can be expressed in a similar format. The appropriate relationship can be developed by combining the following expression for the trajectory of a particle with velocity v,

$$z = z_{vo} + v(t - t_{vo}), \tag{9}$$

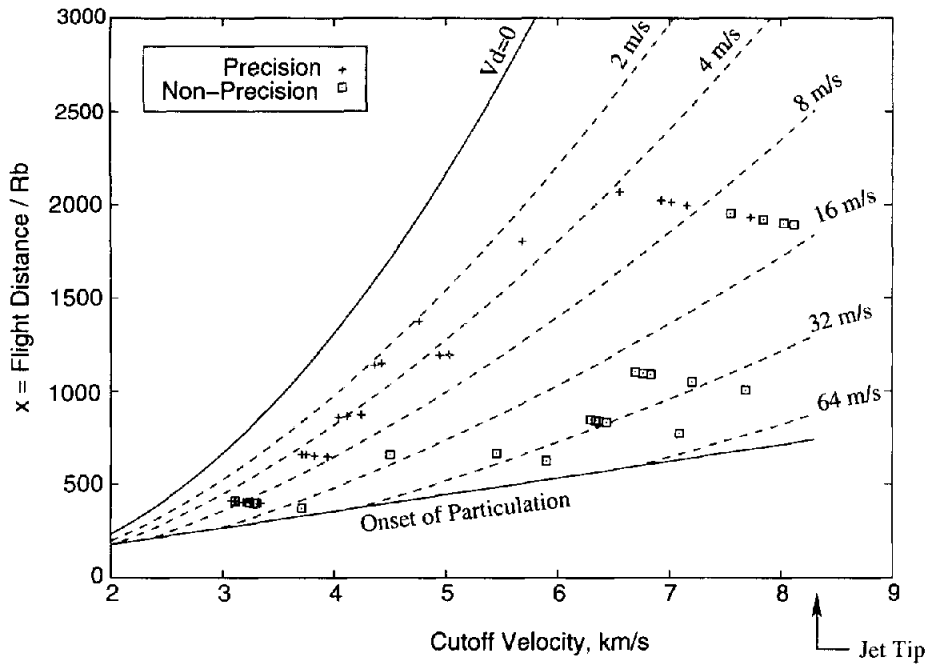

Fig. 6. Normalized flight distance vs. cutoff velocity. The data is for the BRL 3.3 inch standard charge. The curves are for c_b=11.2 m/s, γ=0.94, U_0=900 m/s, and b=0.5.

with Eqns. 4, 5, 7, and 8 to get

$$\frac{v_c}{U_0} - \left[1 + b\frac{v_d}{v_c}x\right]\left[1 + \gamma\frac{c_b}{v_c}x\right] = 0, \tag{10}$$

where

$$x = (z - z_{vo})/r_b \tag{11}$$

is the virtual flight distance of the cutoff particle to the bottom of the hole, normalized to its breakup radius. This expands to a quadratic equation which may be solved for x as a function of v_c. Figure 6 shows this plot for the same data as the previous figure. (Since cutoff velocities were not measured directly in the tests, they have been computed from the penetration depths by assuming hydrodynamic penetration down to cutoff). Only solutions of Eqn. 10 after breakup are applicable; this portion of a (v_c,x) plot can be shown, by combining Eqns. 5, 9, and 11, to be the region of the plane above the line $x = v_c/c_b$. This line is the lower straight line in the plot, and the data points all fall above it, since cutoff is in the particulated mode for all of these tests.

This plot essentially shows the maximum range at which a jet particle remains an effective penetrator, as a function of its velocity, radius, and drift velocity. The significance of the plot is that it provides a method for comparing cutoff data from different devices, along with model predictions, in a common format.

ADDITIONAL COMMENTS

The value for the new parameter, b, used to illustrate the model is, at present, only a rough estimate. But note that b is multiplied by the drift velocity, v_d, in the model, so an error in b simply translates into an error in the drift velocity scale. This means, for example, that if the value of b were halved in the previous example, then Figs. 5 an 6 would remain unchanged except for

the labels on the constant drift velocity curves, which would be doubled. Therefore, if the model is simply being used to correlate data and then make predictions based upon the estimated drift velocities, an error in the value of b is completely unimportant. Only when the drift velocities need to be related to drift measurements or to other models, such as asymmetry models, is the value of b important.

Another issue has to do with particle rotation. Some rotation is induced at breakup, and the magnitude is particularly large in brittle breakup. Modern high precision jets are typically ductile, so the amount of rotation may be relatively low. Therefore, a rotation term may not normally be needed for high precision jets for short to moderate standoff distances. Even so, there will be some standoff distance beyond which the particle rotation angles becomes significant, so beyond that distance the model will overpredict penetration if it is only based upon radial drift. This probably explains why the 25 CD precision data in Fig. 5 appear to have somewhat high drift velocities. The actual standoff distance beyond which rotational effects cannot be ignored depends upon the ductility of the breakup process, the particle sizes, and the aerodynamics of flight.

CONCLUDING REMARKS

There are a variety of circumstances which can lead to jet cutoff, so it should be emphasized that the model described here is intended specifically for cutoff of precision jets during particulated penetration in homogeneous metal targets. For this limited but important set of conditions, the addition of a drift term to the UMIN cutoff model greatly expands its usefulness and provides a very simple and convenient framework for correlating and interpreting penetration data, and for making penetration predictions.

Acknowledgments—The author is grateful to Dan Boeka and Neal Ouye of Primex Technologies and Jim Pearson of *ARDEC* for numerous helpful discussions.

REFERENCES

1. R. DiPersio, J. Simon, and A. Merendino, Penetration of Shaped-Charge Jets into Metallic Targets. BRL Report No. 1296 (1965).
2. M.Held, Evaluation of Shaped Charge Penetration Efficiency by Advanced Diagnostic Techniques, *Proc. 6th Int. Symp. Ballistics*, Orlando, FL, 1981.
3. M.Held, Penetration Cutoff Velocities of Shaped Charge Jets, *Propellants, Explosives, Pyrotechnics* 13, 111-119 (1988)
4. W.P. Walters and J.A. Zukas, *Fundamentals of Shaped Charges*, John Wiley (1989).
5. D.Chi, J. Conner, and R.Jones, A Computational Model for the Penetration of Precision Shaped Charge Warheads, *Proc. 11th Int. Symp. Ballistics*, Brussels, 1989.
6. J.Brown, Modeling and Experimental Studies of a Family of Shaped Charges in a European Collaborative Forum, *Proc. 12th Int. Symp. Ballistics*, San Antonio, TX, 1990.
7. J.P. Curtis, A Stochastic Model of the Penetration of a Shaped Charge Jet into a Semi-Infinite Homogeneous Target, *Proc. 15th Int Symp Ballistics*, Jerusalem, 1995.
8. K.D. Werneyer and F.J. Mostert, Shaped Charge Penetration Prediction with a Statistical Model which Incorporates Radial Velocity Data by Means of Bayes Theorem, *Proc. 18th Int. Symp. Ballistics*, San Antonio, TX, November 1999.
9. M.Held, Characterizing Shaped Charge Performance by Stand-off Behavior, *Proc. of the 7th Int. Symp Ballistics*, Den Haag, 1983.
10. R.D. Boeka, Primex Technologies, San Leandro, California, private communication, to be published.
11. R.Tipton, Cale Users Manual, Lawerence Livermore Laboratory, January 1997.
12. S.L. Hancock, Jet penetration for a class of cumulative mass profiles, *Int. J. Impact Engng.*, 23 (1999) 353-363.
13. James Pearson, ARDEC, private communication.
14. J.N. Majerus and B.R. Scott, CUMIN: A computer code for determining certain jet/target parameters from experimental data. Ballistic Research Laboratory Technical Report, ARBRL-TR-02129 (1978)
15. Ralph E. Shear, Frederick S. Brundick, and John T. Harrison, A link between shaped charge performance and design. Ballistic Research Laboratory Technical Report, ARBRL-TR-02361 (1981)